

Numerical modeling of microwave heating of dielectric materials

E. F. Kent¹ & S. Kent²

¹*Istanbul Technical University, Mechanical Engineering Faculty, Turkey*

²*Istanbul Technical University, Electrical & Electronics Faculty, Turkey*

Abstract

Microwave heating has been established in industry for many years. The temperature distribution within irradiated materials is obtained by determining the electric field distribution. For this reason, modelling the geometry under the plane wave illumination is useful. To determine the temperature distribution, the transmission line analogy for plane wave propagation and reflection for normal incidence angle is used. The heating pattern in a multilayered slab material exposed to a uniform plane wave is obtained. The lossy dielectric object is modelled as an infinitive number of cascaded transmission lines terminated with a metal plate and the inner electric field is calculated.

Keywords: microwave heating, dielectric materials, transmission line model, plane wave.

1 Introduction

This work deals with microwave heating of dielectric lossy materials. Microwave heating has been established in industry for many years. Microwaves are currently used for cooking, baking, drying, melting, sterilising, pasteurising, polymerising, etc. [1-3]. The temperature distribution within irradiated materials is obtained by determining the electric field distribution.

Jansen [4] investigated the reflection and transmission of a plane wave beamed under an angle to a lossy dielectric. Soriano et. al. [5] presented a two-dimensional approach of finite element and finite difference formulation for microwave heating laminar material. A mathematical model for microwave heating of ceramic laminates developed by Pelesko and Kriegsmann [6]. The



transient heat transfer model for selective microwave heating of multilayer material systems was studied by Stern [7].

Lossy dielectric materials have a finite amount of conductivity (σ S/m). At microwave frequencies, this dissipative property is expressed in terms of the material's dielectric loss tangent ($\tan \delta$). The complex permittivity ε is a function of angular frequency ω and can be written as

$$\varepsilon = \varepsilon_0 (\varepsilon' - j \varepsilon'') = |\varepsilon| \exp(-j\delta) = \varepsilon_0 (\varepsilon' - j \sigma / \omega \varepsilon_0) \quad (1)$$

where $\varepsilon_0 = 8.85418 \cdot 10^{-12}$ F/m is the dielectric permittivity of free space, ε' and ε'' are the real and imaginary parts of relative dielectric permittivity. The loss factor of the medium ε'' can be written as

$$\varepsilon'' = \varepsilon' \tan \delta \quad (2)$$

where δ is the dielectric loss angle. The loss tangent is slightly affected by frequency and temperature variations [8].

If the field distribution within the material is known, the heat input due to the microwaves is given as follows [1]

$$P = \sigma |E_i|^2 = \omega \varepsilon_0 \varepsilon'' |E_i|^2 \quad (3)$$

Microwave dissipated power is the source of heat energy induced on the material. The temperature distribution in the material is given by heat transfer equation as

$$\rho C_p \frac{\partial T(\vec{r}, t)}{\partial t} = \nabla \cdot (\kappa \nabla T(\vec{r}, t)) + P(\vec{r}, t) \quad (4)$$

where ρ is the density, C_p the specific heat at constant pressure, κ is the thermal conductivity. For a time harmonic electromagnetic wave, P is constant in time. The inner electric field E_i inside the object is different from the incident field E_{oi} , so it must be calculated by using numerical methods such as ray-optics, geometrical optics [9]-[10], time-domain physical optics (TDPO) [11], time-domain integral equation (TDIE) [12], iterative or variational techniques, moment method [13]-[14], or finite difference time-domain (FDTD) technique [15]. Microwave heating process was studied in recent papers, [16]-[19].

In this paper, to determine the temperature distribution, the transmission line analogy for plane wave propagation and reflection for normal incidence angle is used. If the field distribution within the material is known, the heat input due to the microwaves can be found easily by using various numerical methods. The heating pattern in a multilayered slab material exposed to uniform plane wave is obtained.



2 Numerical modelling of the lossy object

The lossy dielectric object is modelled as an infinitive number of a cascaded transmission line terminated with a metal plate. Let us consider a uniform harmonic plane wave, which illuminates a lossy dielectric object as shown in Figure 1. The permeability of the lossy object is assumed as in free space, i.e. $\mu = \mu_0 = 4\pi \cdot 10^{-7}$ H/m. The object is terminated with a metal plane. The time factor is assumed as $\exp(+j \omega t)$ and depressed.

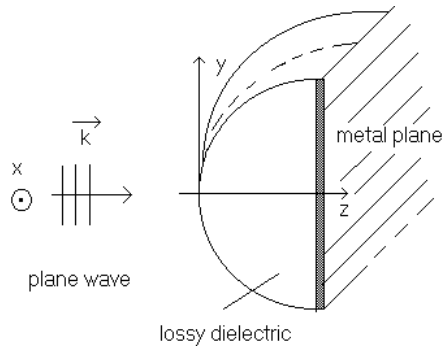


Figure 1: Plane wave illumination of the lossy dielectric object.

For the x-polarized +z travelling wave in an unbounded medium, the incident electric field \mathbf{E}_{oi} has only an x component,

$$\mathbf{E}_{oi} = \mathbf{e}_x E_o \exp(-j \mathbf{k} \cdot \mathbf{r}) \quad (5)$$

where E_o is a constant, \mathbf{k} is the propagation vector in free space,

$$\mathbf{k} = \mathbf{e}_z k_o = \mathbf{e}_z (2\pi / \lambda) \quad (6)$$

k_o is the wave number, λ is the wavelength in free space, and \mathbf{r} is the vector of spatial coordinates. Then, the electric field is expressed as

$$\mathbf{E}_{oi} = \mathbf{e}_x E_o \exp(-j k_o z) \quad (7)$$

It can easily be seen that, this equation satisfies $\nabla \cdot \mathbf{E} = 0$. The associated magnetic field is found according to [20]

$$\mathbf{H} = \mathbf{e}_y (E_o / 120\pi) \exp(-j k_o z) \quad (8)$$

It is well known that, ratios of components of \mathbf{E} to components of \mathbf{H} have the dimensions of impedances and are called wave impedances, $\eta = |\mathbf{E}| / |\mathbf{H}|$.

In this work, the lossy dielectric object is modelled as an infinitive number of cascaded transmission lines as shown in Figure 2.

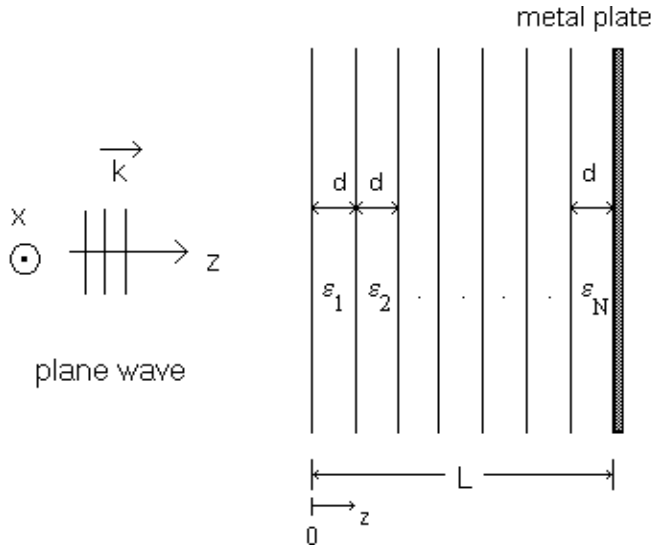


Figure 2: Transmission line model of the lossy object.

In the model we consider the number of lines is being limited as N and the last line is terminated by a perfect conducting metal plate. The total length of the line is L . Each transmission line has a different dielectric permittivity and different characteristic impedance. η_i denotes the characteristic impedance of i -line and is given as

$$\eta_i = |E_i| / |H_i| = \eta_0 / (\epsilon_i)^{1/2} \tag{9}$$

where $\eta_0 \approx 120 \pi \approx 377 \Omega$ is free space intrinsic impedance. The propagation constant γ_i of i -line is

$$\gamma_i = j \omega (\mu_0 \epsilon_i)^{1/2} \tag{10}$$

If we consider the N -layer situation depicted in Figure 2, the uniform plane wave in the free space (ϵ_0, μ_0) impinges normally at the plane boundary with layer-1 (ϵ_1, μ_0) at $z=0$. Layer-1 has a finite thickness and interfaces with layer-2 (ϵ_2, μ_0) at $z=d$, and so on. Reflection occurs at $z=0, z=d, z=2d, \dots$ etc. Assuming $E_0=1$, the total electric field intensity in free space can always be written as the sum of the incident component $\mathbf{e}_x \exp(-j k_0 z)$ and reflected component $\mathbf{e}_x A_1 \exp(j k_0 z)$:

$$\mathbf{E}_0 = \mathbf{e}_x (e^{-jk_0 z} + A_1 e^{jk_0 z}) \tag{11}$$

The magnetic field intensity vector \mathbf{H}_0 in free space that corresponds to the \mathbf{E}_0 in Equation (11) is

$$\mathbf{H}_0 = \mathbf{e}_y \frac{1}{\eta_0} (e^{-jk_0 z} - A_1 e^{jk_0 z}) \tag{12}$$



The electric and magnetic fields in layer-1 can also be represented by combinations of forward and backward waves:

$$\mathbf{E}_1 = \mathbf{e}_x (A_2 e^{-\gamma_1 z} + A_3 e^{\gamma_1 z}) \quad (13)$$

$$\mathbf{H}_1 = \mathbf{e}_y \frac{1}{\eta_1} (A_2 e^{-\gamma_1 z} - A_3 e^{\gamma_1 z}) \quad (14)$$

For N-th layer

$$\mathbf{E}_N = \mathbf{e}_x (A_{2N} e^{-\gamma_N z} + A_{2N+1} e^{\gamma_N z}) \quad (15)$$

$$\mathbf{H}_N = \mathbf{e}_y \frac{1}{\eta_N} (A_{2N} e^{-\gamma_N z} - A_{2N+1} e^{\gamma_N z}) \quad (16)$$

On the right sides of Equations (11)-(16) there are a total of $2N+1$ unknown amplitudes ($A_1, A_2, \dots, A_{2N+1}$). They can be determined by solving the boundary condition equations required by the continuity of the tangential components of the electric and magnetic fields.

$$\begin{aligned} \text{At } z=0, \quad \mathbf{E}_0(0) = \mathbf{E}_1(0), \quad &\rightarrow \quad 1+A_1 = A_2 + A_3 \\ \mathbf{H}_0(0) = \mathbf{H}_1(0), \quad &\rightarrow \quad (1/\eta_0) (1 - A_1) = (1/\eta_1) (A_2 - A_3) \\ \text{At } z=d, \quad \mathbf{E}_1(d) = \mathbf{E}_2(d), \quad &\rightarrow \quad \dots\dots\dots \\ \mathbf{H}_1(d) = \mathbf{H}_2(d), \quad &\rightarrow \quad \dots\dots\dots \\ \dots\dots\dots &\dots\dots\dots \\ \text{At } z=L, \quad \mathbf{E}_N(L) = \mathbf{e}_x (A_{2N} e^{-\gamma_N L} + A_{2N+1} e^{\gamma_N L}) = 0 \\ \mathbf{H}_N(L) = \mathbf{e}_y \frac{1}{\eta_N} (A_{2N} e^{-\gamma_N L} - A_{2N+1} e^{\gamma_N L}) \end{aligned}$$

Arranging the equations in a matrix form, $\mathbf{Ax} = \mathbf{b}$ where \mathbf{x} denotes the vector of unknown amplitudes, $\mathbf{x} = [A_1, A_2, \dots, A_{2N+1}]^T$ and $\mathbf{b} = [-1, -1/\eta_0, 0, 0, \dots, 0]^T$. The superscript T shows the transpose of a column vector, \mathbf{A} is a $2N+1 \times 2N+1$ matrix



$$A = \begin{bmatrix} 1 & -1 & -1 & 0 & \cdot & \cdot & \cdot & 0 \\ -\frac{1}{\eta_0} & \frac{1}{\eta_1} & \frac{1}{\eta_1} & 0 & \cdot & \cdot & \cdot & 0 \\ 0 & e^{-\gamma_1 d} & e^{\gamma_1 d} & -e^{-\gamma_2 d} & -e^{\gamma_2 d} & 0 & \cdot & 0 \\ 0 & \frac{1}{\eta_1} e^{-\gamma_1 d} & -\frac{1}{\eta_1} e^{\gamma_1 d} & -\frac{1}{\eta_2} e^{-\gamma_2 d} & \frac{1}{\eta_2} e^{\gamma_2 d} & 0 & \cdot & \cdot \\ 0 & 0 & 0 & e^{-2\gamma_2 d} & e^{2\gamma_2 d} & -e^{-2\gamma_3 d} & -e^{-2\gamma_3 d} & 0 \\ \cdot & \cdot & \cdot & \frac{1}{\eta_2} e^{-2\gamma_2 d} & -\frac{1}{\eta_2} e^{2\gamma_2 d} & -\frac{1}{\eta_3} e^{-2\gamma_3 d} & \frac{1}{\eta_3} e^{-2\gamma_3 d} & 0 \\ \cdot & \cdot & \cdot & \cdot & \cdot & \cdot & \cdot & \cdot \\ \cdot & \cdot & \cdot & \cdot & \cdot & \cdot & \cdot & \cdot \\ 0 & 0 & \cdot & \cdot & \cdot & 0 & e^{-\gamma_N L} & e^{\gamma_N L} \end{bmatrix}$$

A is a band matrix and invertible. Then, \mathbf{x} can be found as

$$\mathbf{x} = A^{-1} \mathbf{b} \quad (17)$$

and the inner electric field obtained by using these amplitudes for each layer. The input impedance of a transmission line of length L terminated with a Z_L load is given as [21]

$$Z_{in} = \eta \frac{Z_L + \eta \tanh(\gamma L)}{\eta + Z_L \tanh(\gamma L)} \quad (18)$$

The reflection coefficient at any point of the structure can be given by

$$\Gamma = \frac{Z_{in} - \eta}{Z_{in} + \eta} \quad (19)$$

The voltage standing wave ratio SWR is defined as

$$SWR = \frac{|E|_{\max}}{|E|_{\min}} = \frac{1 + |\Gamma|}{1 - |\Gamma|} \quad (20)$$

If the reflection coefficient is small at the surface, in the region external to the material the standing waves will not be observed clearly. The electric fields inside the object will be decreased towards the metal plate. The peaks of the internal standing waves will cause the temperature increase. Temperature increase in the i -th layer is

$$\Delta T = \varepsilon_i'' |E_i|^2 \quad (21)$$



3 Numerical results

The inner electric field for the selected object is found by using a multi-layer modeling of the material. The lossy dielectric object has a decreasing complex permittivity as shown in Figure 3. Each slab has a different dielectric permittivity and different characteristic impedance. Applied frequency is 2.45 GHz, and the number of transmission lines is $N=500$. The length of the material L is chosen as 15 cm, ϵ is chosen as $\epsilon=5.4-j0.00162$ (permittivity of Mica (Ruby) at $T=20^\circ\text{C}$ [8]). Figure 4 shows the normalized electric field distribution and the temperature distribution of the object. The magnitude of the total reflection coefficient is calculated and found as $\Gamma=0.65$.

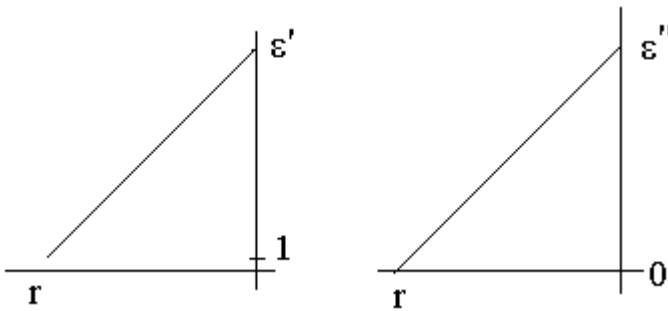


Figure 3: Complex permittivity change of the object.

Figure 5 shows that the corresponding results for Teflon. In this case, $\epsilon=2.1-j0.000315$. The total reflection coefficient is found as $\Gamma=0.15$. For Mica, the temperature distribution reaches the maximum value near the surface and decreases rapidly as it approaches the metal. Five hot spots are observed. In Figure 5 three hot spots are observed. The peak closer to the surface has a higher magnitude.

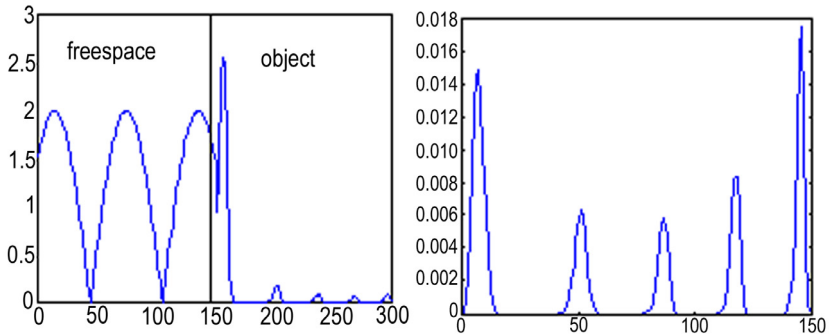


Figure 4: Normalized electric field and temperature distribution for Mica.



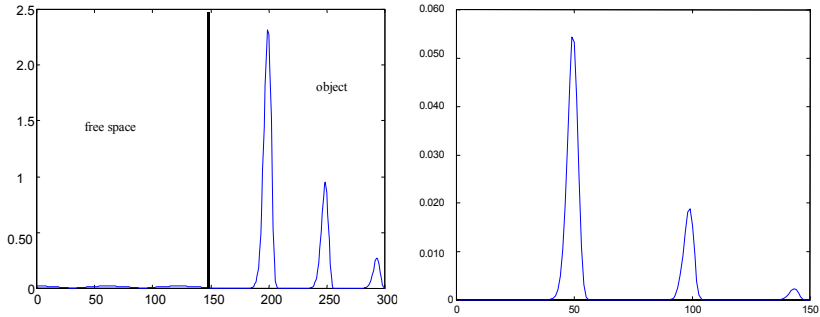


Figure 5: Normalized electric field and temperature distribution for Teflon.

4 Conclusions

In the present work, the temperature distributions are presented for different objects. The obtained results show us if the reflection coefficient is small at the surface, in the region external to the material the standing waves will not be observed clearly. The electric fields inside the object will be decreased towards the metal plate. The peaks of the internal standing waves will cause the temperature increase. The temperature distribution in each layer is found and presented via transmission line method.

References

- [1] Osepchuk, J.M. A history of microwave heating applications. *IEEE Trans. Microwave, Theory and Tech.* **32**, pp. 1200-1224, 1984.
- [2] Stuchly, M.A. & Stuchly, S.S. Industrial, scientific, medical and domestic applications of microwaves. *Proc. IEE-A* **128**, pp. 467-503, 1983.
- [3] Thuéry, J., *Microwaves: Industrial, Scientific and Medical Applications*. Artech House, 1992.
- [4] Jansen, W.J.L., Energy efficient transfer of microwave power to thin lossy dielectrics. *J. Microwave Power* **28(1)**, pp. 45-53, 1993.
- [5] Soriano V., Devece, C. & de los Reyes, E. A finite element and finite difference formulation for microwave heating laminar material. *J. Microwave Power* **33(2)**, pp. 67-76, 1998.
- [6] Pelesko, J.A. & Kriegsmann, G.A. Microwave heating of ceramics. *J. Engineering Mathematics.* **32**, pp. 1-18, 1997.
- [7] Osepchuk, J.M. A history of microwave heating applications. *IEEE Trans. Microwave, Theory and Tech.* **32**, pp. 1200-1224, 1984.
- [8] Stuchly, M.A. & Stuchly, S.S. Industrial, scientific, medical and domestic applications of microwaves. *Proc. IEE-A* **128**, pp. 467-503, 1983.
- [9] Thuéry, J., *Microwaves: Industrial, Scientific and Medical Applications*. Artech House, 1992.



- [10] Jansen, W.J.L., Energy efficient transfer of microwave power to thin lossy dielectrics. *J. Microwave Power* **28(1)**, pp. 45-53, 1993.
- [11] Soriano V., Devece, C. & de los Reyes, E. A finite element and finite difference formulation for microwave heating laminar material. *J. Microwave Power* **33(2)**, pp. 67-76, 1998.
- [12] Pelesko, J.A. & Kriegsmann, G.A. Microwave heating of ceramics. *J. Engineering Mathematics*. **32**, pp. 1-18, 1997.
- [13] Stern, C.H., A transient heat transfer model for selective microwave heating of multilayer material systems. *J. Microwave Power* **33(4)**, pp. 207-215, 1998.
- [14] Rizzi P.A. *Microwave Engineering: Passive Circuits*. Prentice Hall, pp.21-22, 1987.
- [15] Kunz, K.S. & Luebbers, R.J., *The Finite Difference Time Domain Method for Electromagnetics*, CRC Press, Boca Raton, FL, 1993.
- [16] Ma, L., Paul, D.L., Potheary, N., Railton, C., Bows, J., Barratt, L., Mullin, J. & Simons, D., Experimental validation of a combined electromagnetic and thermal FDTD model of a microwave heating process. *IEEE Trans. Microwave, Theory and Tech.* **43(0)**, pp. 2565-2572, 1995.
- [17] Torres, F. & Jacke, B., Complete FDTD analysis of microwave heating processes in frequency-dependent and time dependent media. *IEEE Trans. on Microwave Theory and Techniques*. **45(1)**, pp. 108-117, 1997.
- [18] Nachman, N. & Turgeon, G. Heating pattern in a multi-layered material exposed to microwaves. *IEEE Trans. Microwave, Theory and Tech.* **32**, pp. 547-552, 1984.
- [19] Kent, S. & Kent, E.F., Microwave Heating of Dielectric Objects, *Journal of Microwave Power and Electromagnetic Energy*, **37(2)**, pp. 63-71, 2002.
- [20] Harrington, R.F., *Time Harmonic Electromagnetic Fields*, McGraw Hill, pp. 55-67, 1965.
- [21] Liao, S.Y., *Engineering Applications of Electromagnetic Theory*, West Publishing, pp. 52-84, 1987.

